International Journal of Thermophysics, Vol. 10, No. 3, 1989

A Transient Hot-Wire Method for Measuring the Thermal Conductivity of Gases and Liquids[1]

R. G. Richard[2] and I. R. Shankland[2]

In this paper we describe a version of a transient hot-wire apparatus which employs an integrating digital voltmeter to measure the bridge out-of-balance signal. The integrating period of the voltmeter is variable and is routinely set equal to one 60-Hz power-line cycle, 16.67 ms. Use of measurement or integration periods less than an integral multiple of the power-line period results in substantially more electronic noise and a significant degradation in experimental precision. A correction to the working equation which accounts for the integration of the out-of-balance signal is also presented. The precision of the digital voltmeter used with the apparatus is $\pm 0.1\ \mu$V, which translates into an ultimate precision of ± 0.03 mK in the measured temperature rise. In practice the precision in the temperature rise is typically ± 0.3 mK, which represents a moderate improvement over the precision generally obtained with transient techniques employing automatic bridge balancing schemes. Although the current apparatus is designed principally for measurements of the thermal conductivity of liquids, it can been used for gas-phase measurements, with some decrease in accuracy due to the somewhat larger heat capacity correction which must be applied to the temperature rise measurements. The operation of the instrument was verified by measuring the thermal conductivities of toluene and nitrogen. Preliminary data are presented for the new environmentally acceptable fluorocarbons such as R-134a (CF_3CH_2F), R-123 ($CHCl_2CF_3$), and R-141b (CCl_2FCH_3).

KEY WORDS: chlorofluorocarbons; fluorocarbons; nitrogen; thermal conductivity; toluene; transient hot-wire method.

1. INTRODUCTION

The transient hot-wire technique for measuring the thermal conductivity of fluids has gained acceptance as one of the most reliable and accurate methods of thermal conductivity measurement [1–3]. It is routinely

---

[1] Paper presented at the Tenth Symposium on Thermophysical Properties, June 20–23, 1988, Gaithersburg, Maryland, U.S.A.

[2] Buffalo Research Laboratory, Allied-Signal Inc., Buffalo, New York 14210, U.S.A.

0195-928X/89/0500-0673$06.00/0

employed for thermal conductivity measurements of gases and liquids and is capable of yielding accuracies of a few tenths of 1% [1, 2, 4]. The technique, in all of its variations, is based on the precise determination of the transient temperature rise of a thin wire from measurements of the wire electrical resistance versus time. The thermal conductivity is obtained from the slope of the temperature rise, ΔT, versus $\ln(t)$ curve, which imposes significant constraints on the precision of the ΔT measurements; moreover, the time scale of a typical transient experiment is of the order of 1 s, which places an additional burden on the experimental technique.

In a recent paper, Charitidou et al. [5] summarized three different methods of performing the resistance versus time measurements. The first method utilizes a digital voltmeter in conjunction with a four-terminal technique [6–8] of measuring the wire resistance. The four-terminal technique essentially eliminates the effects at the ends of the wire. The second method [6, 9] eliminates the end effects by incorporating two cells of differing length in a resistance bridge and measures the out-of-balance voltage with a digital voltmeter. The resistance difference of the wires is obtained from the out-of-balance signal and the values of the fixed resistors in the bridge. The rate at which resistance data are acquired using these two techniques varies depending on the actual implementation; e.g., Nagasaka and Nagashima [8], using the four-terminal method, record six resistance values per second, while Roder [9], using the two-cell method, acquires resistance data at 300 measurements per second. As a general rule, increasing the rate of data acquisition by decreasing the time required to perform an individual measurement of ΔT results in an overall loss of precision; for instance, Nagasaka and Nagashima report maximum deviations of 0.2% between measured and fitted temperature rise data, whereas Roder [9, 10] reports maximum deviations of 0.5%. The former measurements were performed with a high-precision integrating digital voltmeter which necessarily acquires data at a slow rate, while Roder employed a very rapid analog-to-digital converter which is influenced by induced electrical noise to a greater extent.

The third method again utilizes two cells in a bridge to compensate for the end effects, but arranges a series of switchable, precision resistors to provide a preset sequence of balance points [11, 12]. The times during the heating cycle at which the bridge attains the preset balance points are measured. This method provides about 6–10 (ΔT, t) measurements per run. Charitidou et al. [5] have modified this technique by using a computer-controlled offset voltage to provide up to 1024 balance points per second. Maximum deviations of no more than 0.08% from the (ΔT, $\ln(t)$) fit were achieved for a temperature rise of 2.5 K.

In this paper, we describe a modified version of the second method, i.e., a two-cell technique employing a voltmeter to measure the bridge out-of-balance signal. We have struck a compromise between the precision of the $[\Delta T, \ln(t)]$ measurements and the rate of data acquisition by using a modern $6\frac{1}{2}$ digit, integrating digital voltmeter which acquires data at a rate of 25 measurements per second. The precision of the voltmeter at this rate is 0.1 μV, which is equivalent to an ultimate precision of 3×10^{-5} K in ΔT; in practice we achieve a precision of 3×10^{-4} K, or equivalently, we observe maximum deviations from the $[\Delta T, \ln(t)]$ line of no more than 0.02% for a 2.5 K temperature rise, which represents an improvement over previously reported experimental precisions.

The cells employed in this work utilize 13-μm-diameter platinum wire and are designed principally for liquid-phase measurements. To confirm the operation of the instrument we present thermal conductivity measurements for toluene. Although not specifically designed for gas-phase measurements, the instrument did perform reasonably well when used to measure the thermal conductivity of nitrogen. Additional gas-phase measurements on fully halogenated chlorofluorocarbons R-11 (CCl_3F) and R-12 (CCl_2F_2) as well as their proposed environmentally acceptable replacements, fluorocarbons R-123 (CCl_2HCF_3), R-141b (CCl_2FCH_3), and R-134a (CH_2FCF_3), are also reported.

2. THE RESISTANCE BRIDGE

A schematic of the bridge circuit is shown in Fig. 1. In this figure, R_1 and R_2 denote the resistance of the short and long cells, respectively, R_3 and R_4 are two precision (± 50 ppm) fixed resistors, and R_5 is a precision ($\pm 0.05\%$) variable resistor. The short and long cells are identical except for their lengths, l_1 and l_2; $l_2 \approx 2l_1$, hence $R_2 \approx 2R_1$. A precision, constant-voltage DC power supply (HP 6200B) energizes the bridge when the mercury-wetted relay is closed. Resistor R_5 is adjusted such that $R_5 = R_1(0) + R_2(0)$ at the beginning of each run, which ensures that the heat flux per unit length, q, remains essentially constant during the run, i.e., when $R_5 = R_1(0) + R_2(0)$ it can be shown by expanding the expression for the heat flux per unit length that

$$q(t) = q(0)\left[1 - \frac{1}{2}\left[\frac{\delta R(t)}{R_1(0) + R_2(0)}\right]^2 + \cdots\right] \tag{1}$$

where

$$\delta R_i(t) = R_i(t) - R_i(0)$$

$$\delta R(t) = \delta R_1 + \delta R_2$$

$$q(0) = \frac{V^2[R_1(0) + R_2(0)]}{(l_1 + l_2)[R_1(0) + R_2(0) + R_5]^2}$$

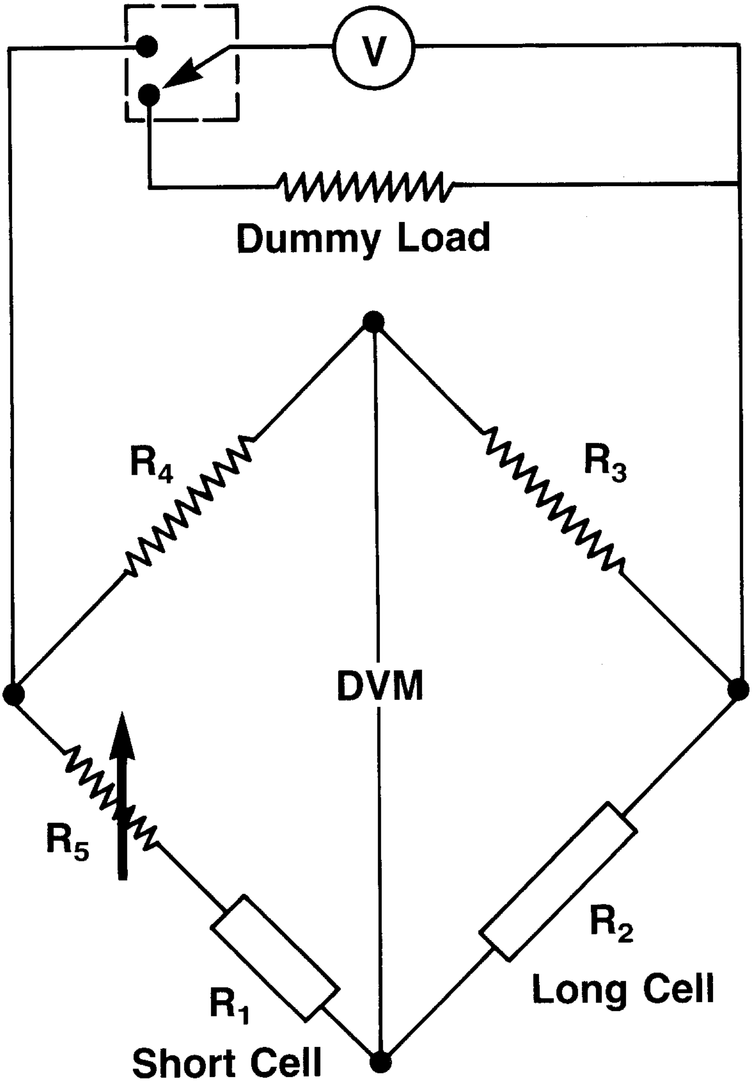

Thermal Conductivity Bridge

Fig. 1. Bridge circuit schematic. V denotes the power supply and DVM represents the digital voltmeter.

In our design, $q(t)$ can be regarded as constant, as it varies by less than 0.02% during a typical run. Equation (1) is similar to the result derived by de Groot et al. [13] for the automatic bridge balancing method.

The fixed resistors in the upper arm of the bridge are chosen such that $R_4{:}R_3$ is 2:1; in the present case $R_4 = 1000\ \Omega$ and $R_3 = 500\ \Omega$. This overall bridge arrangement ensures that $q(t)$ is essentially constant and that the bridge is close to the balance or null position at the start of a run. As R_1 and R_2 increase following initiation of the heating cycle, the bridge deviates from the balance point. The out-of-balance voltage, E, is measured using an integrating digital voltmeter (HP 3456A) which has an input impedance of $10^{10}\ \Omega$. The integration period of the voltmeter is adjustable but is routinely set at 16.67 ms, which is the period of the 60-Hz power lines. A precision of $\pm 0.1\ \mu$V is attainable on the 0–0.1 V DC range with this integration period. Integration of E over an integral multiple of the power-line cycle period effectively eliminates most of the induced 60-Hz noise. This is illustrated in Table I, where a series of E measurements (with the power supply off) is reported. When measurements are performed with integration periods of 16.67 ms and 166.7 ms, the noise, as measured by the standard deviation of the data or the maximum and minimum values, is over an order of magnitude smaller than the noise experienced with an integration period of 1.667 ms.

Although the voltmeter integration period is set to 16.67 ms, we realize only a 40-Hz measurement rate, i.e., one measurement every 25 ms, because the voltmeter requires additional overhead time to complete each voltage measurement. The overall measurement process is best described with reference to Fig. 2, which shows the voltmeter, a multiplexer, and a 10-MHz programmable quartz crystal time base connected to a computer via an IEEE 488 interface bus. The measurement cycle begins with measuring the out-of-balance signal with the relay open—this represents the zero reading of the bridge and is used to correct all subsequent measurements of E. The multiplexer then selects the channel used to measure the power supply voltage, V. A line on a general purpose parallel interface bus is set

Table I. Effect of Voltmeter Integration Period on Signal Noise

Integration period (ms)	No. measurements	Mean (μV)	Min. (μV)	Max. (μV)	SD (μV)
1.667	500	−44.3	−156.	154.	97.
16.67	50	−0.89	−3.7	0.1	0.6
166.7	50	−0.55	−1.0	0.0	0.2

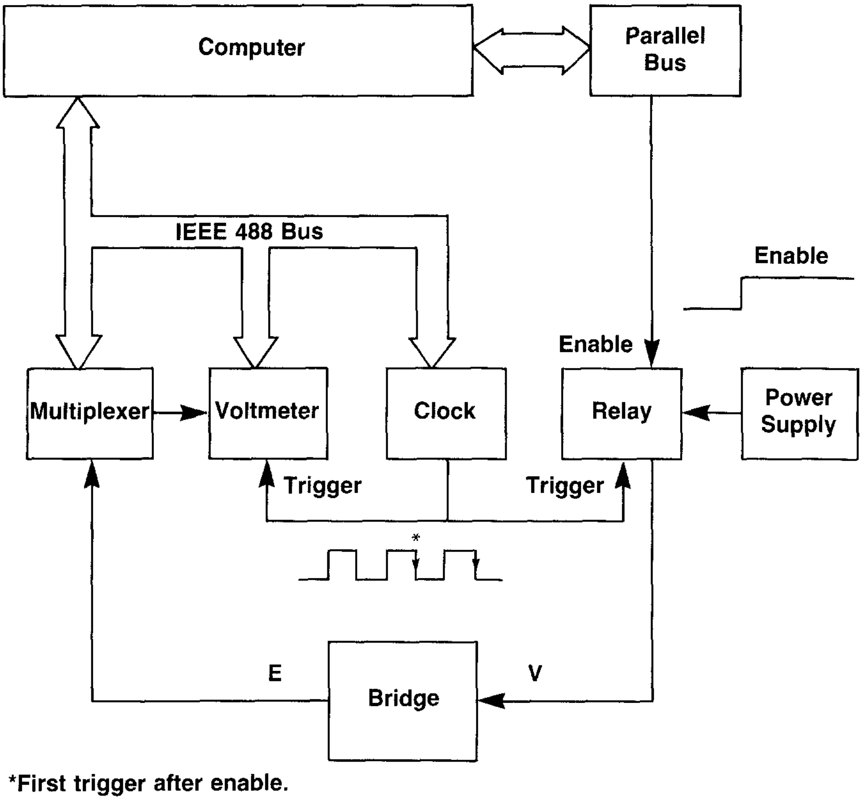

Fig. 2. Measurement cycle schematic.

high in order to enable the relay, which will close when the first falling edge of the clock signal is sensed and will stay closed until the enable line is set low. The same 40-Hz clock signal is connected to the external trigger on the voltmeter which initiates the integration of the out-of-balance voltage every time a falling edge is detected. The relay requires a finite time, 1.21 ± 0.01 ms, to close; all voltmeter trigger times are corrected by this amount. Voltmeter readings are stored in an internal memory and transferred to the computer at the end of the run. The measurement rate is decreased significantly if each reading is transferred to the computer upon its completion.

3. WORKING EQUATIONS

The difference in resistance between the long and the short cells is related to E through

$$\begin{aligned}\Delta R &= R_2 - R_1,\\ &= \frac{R_5[1-(\xi+E^*)]}{[1+\beta(\xi+E^*)]}\end{aligned} \tag{2}$$

where

$$\beta = \frac{\rho+1}{\rho-1} \tag{3}$$

$$E^* = 2E/V \tag{4}$$

$$\xi = \frac{R_4 - R_3}{R_3 + R_4} \tag{5}$$

$$\rho = R_2/R_1 \tag{6}$$

The bridge parameter, β, can also be expressed in terms of the wire lengths:

$$\beta = \frac{l_1 + l_2}{l_2 - l_1} - \frac{2(\rho l_1 - l_2)}{(l_2 - l_1)(\rho - 1)} \tag{7}$$

Since the short and long cells are identical except for their lengths, ΔR corresponds to the resistance of a section of an infinitely long wire [13, 14], $l_2 - l_1$ in length. The temperature rise of the wire, ΔT_w, is derived from its temperature-resistance characteristics and is related to the thermal conductivity of the surrounding fluid, λ, through

$$\Delta T = \Delta T_w + \sum_i \delta T_i \tag{8}$$

$$\Delta T = \frac{q}{4\pi\lambda} \ln(4\kappa t/a^2 C) \tag{9}$$

where a denotes the wire diameter, κ is the thermal diffusivity of the fluid, and C is Euler's constant. The small correction terms, δT_i, defined previously [13], and other corrections arising from slight differences in the resistance per unit length of the wires [14] are applied to ΔT_w.

Because we integrate the out-of-balance signal over a time interval Δt, we measure $\bar{E}$:

$$\bar{E} = \frac{1}{\Delta t} \int_{t_i}^{t_i + \Delta t} E(t)\, dt \tag{10}$$

which can be identified with the instantaneous value of E at some time $t_i + \delta t$, where $\delta t < \Delta t$. Here t_i is the time the voltmeter reading is triggered. The time correction, δt, can be obtained to sufficient precision by integrating

$$E^*(t) = \frac{R_5 - \Delta R(t)}{R_5 + \beta\, \Delta R(t)} - \xi \tag{11}$$

where

$$\Delta R(t) = \Delta R(0)[1 + \bar{\alpha}\, \Delta T_{\mathrm{w}}] \tag{12}$$

and ΔT_{w} is approximated using Eq. (9). Here $\bar{\alpha}$ is the effective linear resistance temperature coefficient for the platinum wire. The result for the time correction is

$$\delta t = \left(\frac{\Delta t}{2}\right)\left[1 - \left(\frac{1+\gamma}{3}\right)\frac{\Delta t}{t_i}\right] \Big/ \left[1 - \left(\frac{1+\gamma}{2}\right)\frac{\delta t}{t_i}\right] \tag{13}$$

where

$$\gamma = \frac{2\bar{\alpha} q \beta\, \Delta R(0)}{4\pi\lambda[R_5 + \beta\, \Delta R(t)]} \tag{14}$$

To a very good approximation the time correction is given by $\delta t = \Delta t/2$, which holds to better than 0.01% in our apparatus.

4. THERMAL CONDUCTIVITY CELLS

Figure 3 illustrates the construction of the cells. The two platinum wires, differing only in length, were mounted in the cells and tensioned using a spring mechanism similar to that employed by Kestin et al. [1]. Cylindrical cells were formed from semicylindrical channels machined into two blocks of 316 stainless steel. The cell assembly is contained in a pressure vessel fitted with electrical feed-throughs, a platinum resistance thermometer, and a connection to a pressure transducer. Temperature control is maintained by placing the vessel in an air bath controlled to ±0.05°C; temperature variations within the cells themselves are much less than this due to the damping effect of the steel body.

The platinum wires were annealed before tensioning and then calibrated *in situ* using the bridge in a steady-state mode to measure ΔR. The capability of the voltmeter to measure the ratio of two resistances directly was employed for measuring $\rho = R_2/R_1$. Both quantities were

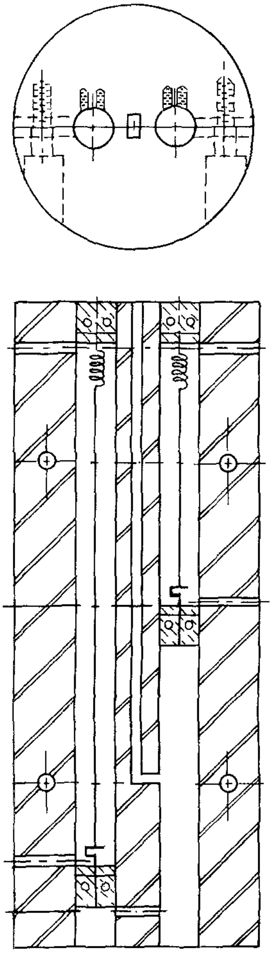

Fig. 3. Cell construction. Cell block is contained in a thermostated pressure vessel (not shown).

measured at different steady-state heat fluxes and extrapolated to zero heat flux. The variation of ρ with temperature is very small, changing by 0.12% over a 50 K change in temperature.

5. EXPERIMENTAL PRECISION

Major sources of measurement error in λ can be divided into three groups: the first source of error consists of the effects of uncertainties in the measured quantities E, V, and t; the second group consists of errors caused by uncertainty in the wire properties $\bar{\alpha}$ and $l_2 - l_1$; and the third group of errors stems from systematic errors in the bridge parameters ξ, R_5, and ρ. There are other sources of error arising from approximations made in the corrections to the working equation and from imperfect end-effect compensation; these and other similar sources of error are not discussed here.

As mentioned previously, we achieve a precision of $\pm 1\ \mu$V in E, which corresponds to about ± 0.3 mK in ΔT_w. The uncertainty associated with measuring V is about 0.01%, which translates to about ± 0.2 mK in ΔT_w. Time measurements are uncertain to the extent of about ± 0.02 ms, which stems primarily from the uncertainty in the relay closing time. The overall contribution of the first group of errors is about ± 0.5 mK (typically ± 0.02%) in ΔT_w.

Uncertainties in the wire properties $\bar{\alpha}$ and $l_2 - l_1$ cause a similar relative error in λ. Calibration of the wire resistance yielded $\bar{\alpha}$ to about ± 0.1%, while the uncertainty in the measurement of l_1 and l_2 could cause a ± 0.1% error in $l_2 - l_1$. Consequently, λ is burdened with a possible ± 0.2% uncertainty from these two sources.

Errors in the bridge parameters will cause systematic errors in ΔT_w which, if time dependent, lead to systematic errors in λ. The easiest to treat is the error caused by an uncertainty in R_5. Differentiating the bridge equation, Eq. (2), shows that a 0.05% error in R_5 produces the same error in λ. This experimental error does not introduce curvature into the $[\Delta T, \ln(t)]$ line, but just shifts the slope. A conservative 0.05% uncertainty in β (through the measurement of ρ) produces a systematic error of 0.3 mK in ΔT_w. This particular error is time dependent, which will lead to curvature of the $[\Delta T, \ln(t)]$ line; however, the deviation from linearity is much smaller than 0.1 mK for a typical experiment. An error in ξ (i.e., in R_3 and R_4) has a similar effect, except its magnitude is much smaller, as R_3 and R_4 are known to within ± 50 ppm.

Evidence supporting operation of the instrument in accordance with the working equations, as well as evidence of the claimed precision in the measurement of ΔT_w, is shown in Fig. 4. This plot depicts the deviations between the corrected, measured temperature rise data and the fitted values for two runs performed on N_2 at 313 K using a 4 K temperature rise. There is no systematic trend evident in the deviation plot and the magnitude of the largest single deviation is about 1 mK, or about 0.03% of the temperature rise.

The total effect of the aforementioned errors is reflected in a possible ± 0.4% inaccuracy in λ. This estimate is commensurate with the agreement between results of test measurements performed on N_2 and toluene and previously published thermal conductivity data for these fluids. Nitrogen

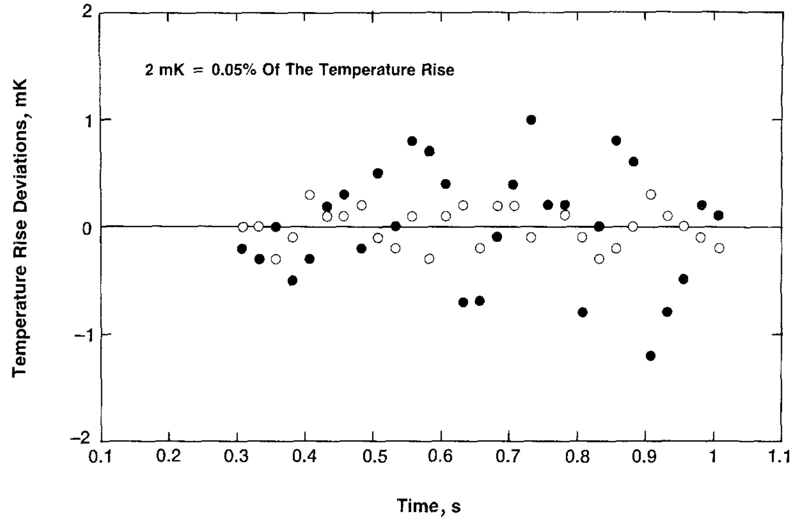

Fig. 4. Deviations between measured and fitted ΔT data for two runs (open and filled circles) in N_2 at 313 K using a 4 K temperature rise.

data, extrapolated to zero density, are given in Table II. This table also summarizes the differences between the present measurements and linear interpolations of the data reported by Maitland et al. [15]; the average discrepancy between the two sets of data is 0.3%. Thermal conductivity data for tuluene are listed in Table III. Deviations between these data and the correlation of Nieto de Castro et al. [3] are also given in Table III. The average absolute discrepancy in this case is 0.7%, which is within the mutual uncertainties of the present measurements and the correlation. No evidence of radiation affecting the measured toluene thermal conductivities [4] was detected.

Table II. Zero-Density N_2 Thermal Conductivity Data

T (K)	λ^0 ($\mathrm{mW \cdot m^{-1} \cdot K^{-1}}$)	$[(\lambda^0 - \lambda^0_{[15]})/\lambda^0_{[15]}] \times 100$ (%)[a]
310.15	26.75	0.27
313.15	26.91	0.07
323.15	27.69	0.29
333.15	28.43	0.27
343.15	29.19	0.54
352.15	29.53	−0.50
Ave. abs. deviat.		0.30

[a] Data taken from Ref. 15: $\lambda^0_{[15]} = 24.031 + 0.07152\ (T - 273.15)$.

Table III. Toluene Thermal Conductivity Data

T (K)	λ ($mW \cdot m^{-1} \cdot K^{-1}$)	$[(\lambda - \lambda_{[3]})/\lambda_{[3]}] \times 100$ (%)[a]
311.15	126.3	−0.68
323.15	123.3	−0.25
333.15	121.3	0.62
343.15	119.0	1.20
Ave. abs. deviat.		0.7

[a] $\lambda_{[3]}$ data taken from Ref. 3, Eq. (8).

6. FLUOROCARBON VAPOR THERMAL CONDUCTIVITIES

Chlorofluorocarbons, especially R-11 and R-12, have been widely utilized in modern society as working fluids in refrigeration and air conditioning equipment and as expansion agents for a variety of foamed polymeric materials which are useful as thermal insulation materials. The wide application of these fluids is a consequence of their unique combination of thermophysical properties and other properties such as nonflammability, low toxicity, and good chemical stability. However, when released into the atmosphere these molecules have proven to be so stable that the major known removal mechanism from the environment is photolytic breakdown in the stratosphere. The most promising environmentally acceptable replacements for these molecules are R-134a, to replace R-12, and R-123 and/or R-141b, to replace R-11. We have used the apparatus

Table IV. R-12 and R-134a Zero-Density Thermal Conductivity

R-12				R-134a	
T (K)	λ^0 ($mW \cdot m^{-1} \cdot K^{-1}$)	δ_T[a] (%)	δ_M[b] (%)	T (K)	λ^0 ($mW \cdot m^{-1} \cdot K^{-1}$)
30.0	10.26	−3.9	−2.2	30.0	14.50
35.0	10.54	−4.1	−2.4	40.0	15.26
38.0	10.69	−4.0	−2.4	50.0	16.15
44.0	11.01	−4.1	−2.5	60.0	17.26
49.0	11.29	−4.1	−2.7	70.0	18.27
55.0	11.63	−3.8	−3.0		

[a] Deviation from the correlation of Touloukian [16], $\delta_T = [(\lambda_{corr} - \lambda_{meas})/\lambda_{meas}] \times 100$.

[b] Deviation from the correlation of Makita et al. [17], $\delta_M = [(\lambda_{corr} - \lambda_{meas})/\lambda_{meas}] \times 100$.

described here to measure the vapor-phase thermal conductivity of R-12, R-134a, R-11, R-123, and R-141b over a small range of temperatures. To our knowledge these are the first reported data for these fluorocarbons using a transient hot-wire technique. The data are preliminary and measurements over a broader temperature range as well as measurements of the thermal conductivity of the liquids are planned.

Zero-density thermal conductivity data for R-12 and R-134a are summarized in Table IV. Measurements were performed over a small range of pressures (limited by the saturation pressure) and the data extrapolated to zero density. Because the data were obtained at relatively low densities, they do not enjoy the accuracy of measurements taken at higher densities owing to higher heat capacity corrections [13] and possible Knudsen effects [13]. We estimate the accuracy to be of the order of ±2%. Deviations between the present measurements and the correlations of Touloukian [16] and Makita et al. [17] are also listed in Table IV. The Touloukian correlation is consistently about 4% lower than the present measurements. The data of Makita et al. are estimated to have an accuracy of ±2% and agree with this work within the mutual limits of uncertainty.

The data shown in Table IV indicate that R-12 and R-134a vapor thermal conductivities differ by about 40%. This may not be significant as far as application as a refrigerant working fluid is concerned, where the thermal conductivity of the liquid is a more important property, but it will have a significant effect on the application of R-134a as a foam expansion agent, where the thermal insulation characteristics of the expansion gas are an important factor in determining the overall thermal insulation properties of low-density foams.

Table V contains thermal conductivity data for R-11, R-123, and R-141b which were measured at pressures just below the saturation

Table V. R-11, R-123, and R-141b Vapor Thermal Conductivity

R-11			R-123		R-141b	
T (K)	λ (mW·m^{-1}·K^{-1})	δ_T[a] (%)	T (K)	λ (mW·m^{-1}·K^{-1})	T (K)	λ (mW·m^{-1}·K^{-1})
305.15	8.57	−5.4	306.15	11.07	284.15	9.01
308.15	8.81	−6.6	308.15	11.31	293.15	9.45
313.15	9.11	−7.5	313.15	11.76	303.15	10.53
318.15	9.36	−7.8	318.15	12.14	313.15	11.34
323.15	9.61	−8.2	323.15	12.60	323.15	11.89
328.15	9.86	−8.6	328.15	13.02	333.15	12.53

[a] Deviation from the correlation of Touloukian [16], $\delta_T = [(\lambda_{corr} - \lambda_{meas})/\lambda_{meas}] \times 100$.

pressure of these fluids. These data are probably accurate only to ±3% as they were determined at quite low number densities. The deviations between the present measurements and the correlation of Touloukian [16] are given in Table V; the measurements are from 5 to 8% higher than the correlation. The major use of R-11 is as an expansion agent for the manufacture of rigid polyurethane and polyisocyanurate foams which are used as high-efficiency thermal insulation materials. Substitution of either R-123 or R-141b, with higher vapor thermal conductivities, for R-11 will degrade the overall insulation characteristics of the foam material if all other aspects of the foam structure are kept constant.

ACKNOWLEDGMENT

The authors thank Allied-Signal Inc. for permission to publish this work.

REFERENCES

1. J. Kestin, R. Paul, A. A. Clifford, and W. A. Wakeham, *Physica* **100A**:349 (1980).
2. M. J. Assael, M. Dix, A. Lucas, and W. A. Wakeham, *J. Chem. Soc. Faraday Trans. I* **77**:439 (1981).
3. C. A. Nieto de Castro, S. F. Y. Li, A. Nagashima, R. D. Trengove, and W. A. Wakeham, *J. Phys. Chem. Ref. Data* **15**:1073 (1986).
4. C. A. Nieto de Castro, S. F. Y. Li, G. C. Maitland, and W. A. Wakeham, *Int. J. Thermophys.* **4**:311 (1983).
5. E. Charitidou, M. Dix, M. J. Assael, C. A. Nieto de Castro, and W. A. Wakeham, *Int. J. Thermophys.* **8**:511 (1987).
6. N. Mani, Ph.D. thesis (University of Calgary, Calgary, Canada, 1971).
7. Y. H. Julia, J. F. Renaud, D. J. Ferrand, and P. F. Malbrunot, *Rev. Sci. Instrum.* **48**:1654 (1977).
8. Y. Nagasaka and A. Nagashima, *Rev. Sci. Instrum.* **52**:229 (1981).
9. H. M. Roder, *J. Res. Natl. Bur. Stand. (U.S.)* **86**:457 (1981).
10. H. M. Roder, *J. Res. Natl. Bur. Stand. (U.S.)* **87**:279 (1982).
11. G. P. Anderson, J. J. de Groot, J. Kestin, and W. A. Wakeham, *J. Phys. E Sci. Instrum.* **7**:948 (1974).
12. C. A. Nieto de Castro, J. C. G. Colado, W. A. Wakeham, and M. Dix, *J. Phys. E Sci. Instrum.* **9**:1073 (1976).
13. J. J. de Groot, J. Kestin, and H. Sookiazian, *Physica* **75**:454 (1974).
14. J. Kestin and W. A. Wakeham, *Physica* **92A**:102 (1978).
15. G. C. Maitland, M. Mustafa, and W. A. Wakeham, *J. Chem. Soc. Faraday Trans. I* **79**:163 (1983).
16. Y. S. Touloukian (ed.), *Thermophysical Properties of Matter, Vol. 3. Thermal Conductivity Nonmetallic Liquids and Gases*, (Plenum, New York, 1970), pp. 185–189.
17. T. Makita, T. Tanaka, Y. Morimoto, M. Noguchi, and H. Kubota, *Int. J. Thermophys.* **2**:249 (1981).